

A search for shocked quartz grains in the Allerød-Younger Dryas boundary layer

Annelies VAN HOESEL^{1,2*}, Wim Z. HOEK², Gillian M. PENNOCK¹, Knut KAISER³,
Oliver PLÜMPER¹, Michal JANKOWSKI⁴, Maartje F. HAMERS¹, Norbert SCHLAAK⁵,
Mathias KÜSTER⁶, Alexander V. ANDRONIKOV⁷, and Martyn R. DRURY¹

¹Department of Earth Sciences, Utrecht University, Budapestlaan 4, 3584 CD Utrecht, The Netherlands

²Department of Physical Geography, Utrecht University, Heidelberglaan 2, 3584 CS Utrecht, The Netherlands

³GFZ German Research Centre for Geosciences, Telegrafenberg, 14473 Potsdam, Germany

⁴Department of Soil Science and Landscape Management, Nicolaus Copernicus University, Gagarina 9a, 87-100 Toruń, Poland

⁵State Agency for Mining, Geology and Resources Brandenburg (LBGR), Inselstrasse 26, 03046 Cottbus, Germany

⁶Institute of Geography and Geology, University of Greifswald, Friedrich-Ludwig-Jahn Strasse 16, 17487 Greifswald, Germany

⁷Lunar and Planetary Laboratory, University of Arizona, Tucson, Arizona 85721, USA

*Corresponding author. E-mail: vanhoesel.geo@gmail.com

(Received 08 March 2014; revision accepted 13 January 2015)

Abstract—The Younger Dryas impact hypothesis suggests that multiple airbursts or extraterrestrial impacts occurring at the end of the Allerød interstadial resulted in the Younger Dryas cold period. So far, no reproducible, diagnostic evidence has, however, been reported. Quartz grains containing planar deformation features (known as shocked quartz grains), are considered a reliable indicator for the occurrence of an extraterrestrial impact when found in a geological setting. Although alleged shocked quartz grains have been reported at a possible Allerød-Younger Dryas boundary layer in Venezuela, the identification of shocked quartz in this layer is ambiguous. To test whether shocked quartz is indeed present in the proposed impact layer, we investigated the quartz fraction of multiple Allerød-Younger Dryas boundary layers from Europe and North America, where proposed impact markers have been reported. Grains were analyzed using a combination of light and electron microscopy techniques. All samples contained a variable amount of quartz grains with (sub)planar microstructures, often tectonic deformation lamellae. A total of one quartz grain containing planar deformation features was found in our samples. This shocked quartz grain comes from the Usselo palaeosol at Geldrop Aalsterhut, the Netherlands. Scanning electron microscopy cathodoluminescence imaging and transmission electron microscopy imaging, however, show that the planar deformation features in this grain are healed and thus likely to be older than the Allerød-Younger Dryas boundary. We suggest that this grain was possibly eroded from an older crater or distal ejecta layer and later redeposited in the European sandbelt. The single shocked quartz grain at this moment thus cannot be used to support the Younger Dryas impact hypothesis.

INTRODUCTION

In 2007, it was suggested that one or more extraterrestrial impacts or airbursts caused the onset of the Younger Dryas cold period (12.85–11.65 ka), megafaunal extinctions, and a decline in human population (Firestone et al. 2007; Wittke et al. 2013). This idea is also known as the Younger Dryas impact hypothesis and was initially based on elevated concentrations (compared to

background) of several markers in the Allerød-Younger Dryas boundary (~12.85 ka) at sites in North America and one in Europe. These markers include, among others, magnetic spherules, nanodiamonds, lechatelierite, and platinum group elements (Firestone et al. 2007; Kennett et al. 2009a, 2009b; Bunch et al. 2012; Petaev et al. 2013). However, the Younger Dryas impact hypothesis has been severely criticized because not all of the reported markers were independently reproducible, nor were the markers

considered as diagnostic evidence for an impact and/or found at well-dated sites. The general consensus is therefore that evidence for the hypothesis is still missing (French and Koeberl 2010; Pinter et al. 2011; Van Hoesel et al. 2014; Meltzer et al. 2014).

Planar deformation features (PDFs) are thin ($<1\ \mu\text{m}$), closely spaced ($<10\ \mu\text{m}$), straight, parallel deformation planes in crystals, which form during shock deformation (e.g., Langenhorst 2002; French and Koeberl 2010). PDFs are unique shock-related features, and shocked quartz is therefore widely used as a reliable impact indicator, although these have also been created artificially in shock-wave experiments and nuclear explosions (French and Koeberl 2010). In addition, the orientation and number of sets within one grain is related to shock pressure and can thus give information about the impact itself (Grieve et al. 1996). Although PDFs are amorphous in origin, these amorphous PDFs can heal, or recrystallize, in the presence of water and high temperatures; the healed PDFs can be observed in light microscopy as traces of fluid inclusions (Goltrant et al. 1991; Leroux and Doukhan 1996; Trepmann and Spray 2006). Using light microscopy, PDFs can often be easily identified. Other, nonshock features (e.g., tectonic deformation lamellae or growth features), however, can have somewhat similar appearances in light microscopy and might be mistaken for PDFs (Table 1) (French and Koeberl 2010; Reimold et al. 2014). Other methods, such as transmission electron microscopy (TEM), light microscopy using a universal or spindle stage, or scanning electron microscopy (SEM) cathodoluminescence (CL) imaging of sectioned grains are thus necessary to confirm the true nature of planar deformation features (Bohor et al. 1987; Goltrant et al. 1991; Ferrière et al. 2009; French and Koeberl 2010; Hamers and Drury 2011). Mahaney et al. (2010a) report finding PDFs in quartz in an undated black mat-like layer in the Venezuelan Andes, reported as representing the Allerød-Younger Dryas boundary. However, Mahaney et al. (2010a) only imaged whole grains using SEM, showing parallel surface features spaced $0.5\text{--}1.0\ \mu\text{m}$ apart. Although the spacing of these features is consistent with the spacing of PDFs, more information is necessary to distinguish these features from nonshock features. Thus, based on the current evidence these grains cannot be considered to be shocked quartz. Moreover, in a follow-up study on the same site Mahaney et al. (2010b) reported that they found no irrefutable PDFs and focused instead on the presence of closely spaced fractures that were oriented parallel to the surface of the quartz grains, highly disrupted grain surfaces, and extreme brecciation. These features, however, are not considered as indicative of high shock pressures (French and Koeberl 2010).

The presence of extensive shocked quartz grains at the Allerød-Younger Dryas boundary would be a clear indication that an extraterrestrial impact occurred around the time of the proposed Younger Dryas impact event. This is especially the case if it can be shown that the grains contain mostly amorphous or fresh PDFs, which can be indicative of relatively young impact layers that have experienced limited postimpact alteration (Trepmann and Spray 2006; French and Koeberl 2010). Although fresh-looking PDFs have also been found in older craters (Holm et al. 2011), PDFs that appear fresh in light microscopy might prove to be decorated when using higher resolution imaging techniques such as SEM (Alwmark 2009). An absence of shocked quartz grains, on the other hand, does not dismiss the impact hypothesis, since no shocked quartz is expected if the proposed Younger Dryas impact event consisted of airbursts, or hit the ice sheet or occurred over the ocean. To test the Younger Dryas impact hypothesis, we investigated several palaeosols of Allerød-Younger Dryas age for the occurrence of shocked quartz grains using transmission light microscopy (TLM), new scanning electron microscopy methods involving cathodoluminescence (SEM-CL), and electron backscattered diffraction (EBSD) and transmission electron microscopy (TEM). The SEM-CL imaging is particularly useful for distinguishing deformation lamellae and planar deformation features.

STUDY AREAS

Confirmation that an impact caused climate change or an extinction event depends on timing, that is, there must be a clear and causal relationship between the timing of the event and the supposed impact (Van Hoesel et al. 2014). Therefore, we investigated samples from the Allerød-Younger Dryas boundary at nine relatively well-dated locations in the European coversand area, and one from a black mat deposit in North America (Figs. 1 and 2; Table 2). A detailed description of these sites can be found in Data S1 of supporting information. Additional radiocarbon ages were obtained for three of the sites in this study (Table 3).

In the coversand area, the Allerød-Younger Dryas boundary is often marked by either the Usselo or Finow palaeosol (Hijzeler 1947; Schlaak 1993; Kasse 2002; Kaiser et al. 2009). The formation of both types of soils is thought to have started during the Allerød, when aeolian activity ceased and the landscape stabilized, and continued until the soil was buried by renewed aeolian activity during the Younger Dryas cold period (Kaiser et al. 2009). In the wetter parts of the landscape, peat started to develop during the Allerød, which formed layers that were also subsequently buried during the Younger Dryas (Kaiser et al. 2006). Both the

Table 1. Properties of PDFs compared to other planar fractures and non-shock features.^a

	Planar deformation features	Planar fractures	Tectonic deformation lamellae	Growth lines
Shape	Straight, parallel	Straight, parallel	Often slightly curved	Straight, parallel, sometimes with zigzag
Width	<2–3 μm (typically <1 μm)	3–10 μm	>2 μm (typically $\geq 10\text{--}20$ μm)	Narrow
Spacing	<10 μm (typically <2 μm)	>15 μm	>5 μm	Close, irregular
Sets/grain	≥ 1 (typically >3)	1–3	1–2 (typically 1)	1
Orientation	Parallel to specific crystallographic planes	Parallel to specific crystallographic planes	Broad range of low angles to basal plane	Parallel to crystallographic planes that are not typical for PDFs
CL imaging	Red/nonluminescent sharp/well defined		Red/blue luminescent hard to define	
Shock pressure	10–30 Gpa	5–20 Gpa	na	na

^aBased on French and Koeberl (2010), Hamers and Drury (2011), and Grieve et al. (1996).

na = not applicable.

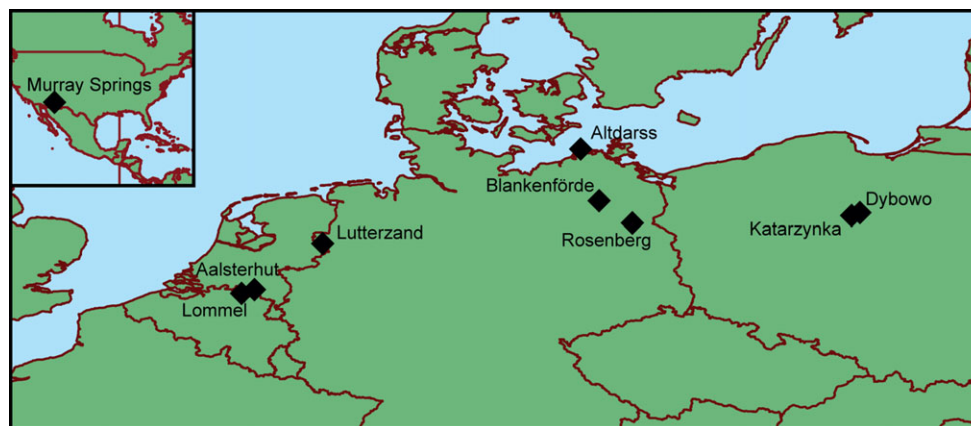


Fig. 1. Location of the field sites in Europe and North America (inset).

Usselo and Finow buried soils and the sampled peat layers would have been at the surface at the time of the proposed Younger Dryas impact event and should thus have collected any impact-related material. Any material found, however, could have been incorporated in the soils at any time during their formation period and analysis of these buried soils will thus only give a first indication of the possibility of an impact at the onset of the Younger Dryas. The North American Black Mat differs in that respect. These wet soils and algal mats did not form until the start of the Younger Dryas (Haynes 2008), and the Black Mat would thus cover any material related to the Younger Dryas impact event. Three of the sites in this study have been previously investigated for impact markers (Firestone et al. 2007; Tian et al. 2011; Van Hoesel et al. 2012), namely Murray Springs (Arizona, USA), Lommel Maatheide (Belgium), and Geldrop Aalsterhut (the Netherlands).

METHODS

At each site, one or more sediment samples (Table 2) were taken from the Allerød-Younger Dryas boundary layer. Samples (containing roughly 150 g of sediment) from each site were treated with HCl, H₂O₂, and/or repeated rinsing to remove carbonates and organic matter when necessary, and sieved to remove the smallest (<20 μm) and largest grains (>500 μm). To isolate the quartz grains, density separation was performed using a Loc50 centrifuge and diiodemethane heavy liquid (of 2.62, 2.64, 2.66 g cm⁻³) at the Mineral Separation Laboratory at the VU Amsterdam. As most samples were rich in quartz grains and knowing that shocked quartz can have a slightly lower density than unshocked quartz grains (Langenhorst and Deutsch 1994), the 2.62–2.64 g cm⁻³ fraction was used for further analysis. Due to the overlapping densities of different minerals, this fraction can also contain minor

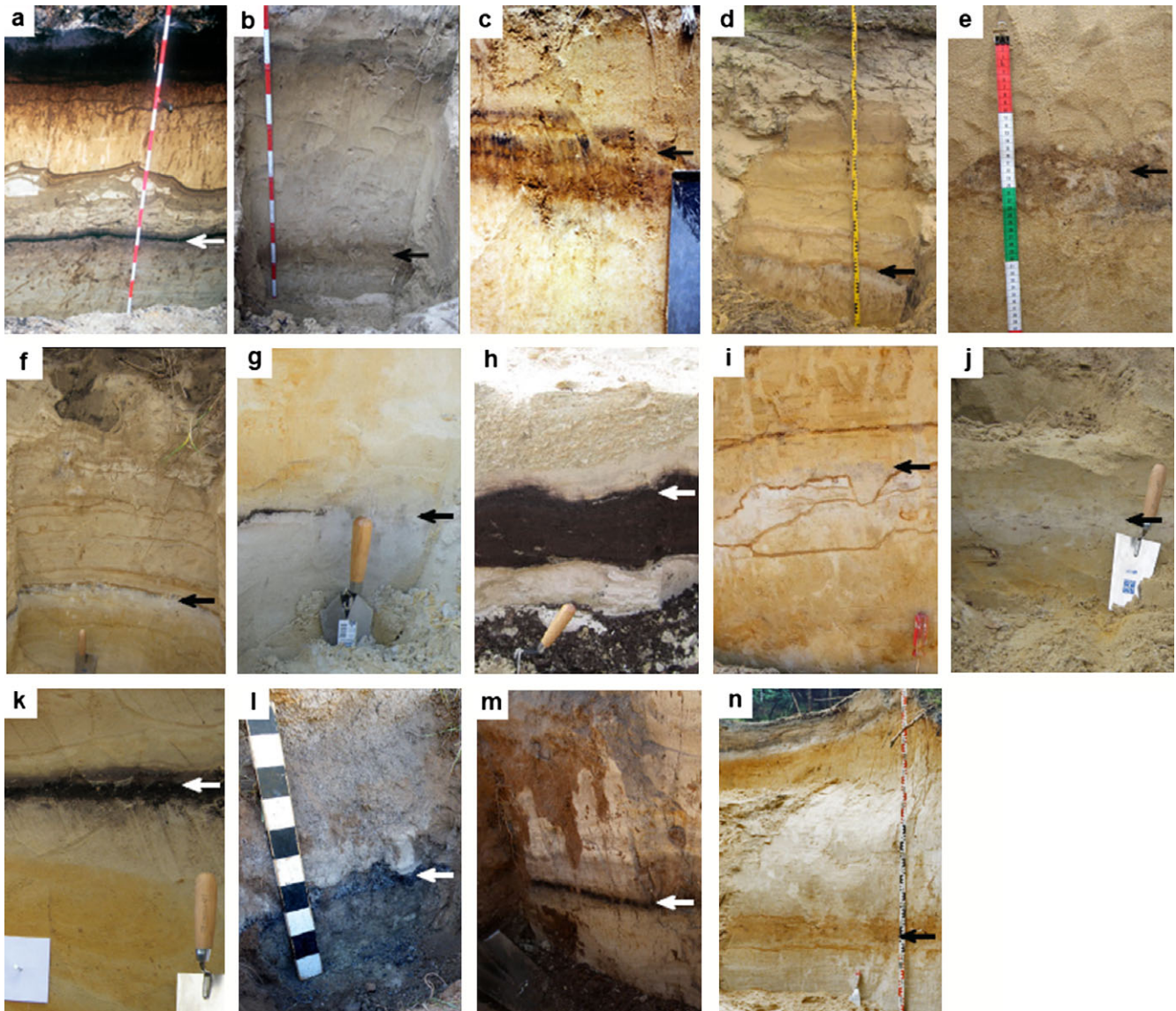


Fig. 2. Photos of sampled layers at the field locations given in Fig. 1. Arrows indicate the location of the sampled layers (a). Thin Allerød peat layer at Altdarss. b) Finow palaeosol at Blankenförde. c) Finow palaeosol at Dybowo. d) Usselo palaeosol at Geldrop Aalsterhut. e) Finow palaeosol at Katarzynka. f) Usselo palaeosol at Katarzynka. g) Usselo palaeosol at Lommel Maatheide. The Usselo palaeosol is visible as gray specks and a thin black organic rich layer in the top of the white coversand. h) Thick Allerød peat bed at Lommel Maatheide. The undulating top of the peat suggests that the layer has been eroded. i) Usselo palaeosol at Lommel Maatheide. j) Usselo palaeosol at Lutterzand. This palaeosol was not sampled but only used for radiocarbon dating. k) Thin Allerød peat layer at Lutterzand. l and m) Black Mat at Murray Springs. n) Finow palaeosol at Rosenberg.

amounts of feldspar. Subsamples of the $2.62\text{--}2.64\text{ g cm}^{-3}$ fraction were embedded in epoxy resin (Epotek 301) using 1.27 and 2.54 cm diameter molds. The resulting 5 mm thick sections were subsequently polished to a $1\text{ }\mu\text{m}$ finish with Al_2O_3 using standard polishing procedures. Each polished section contained at least 1500 grains. The number of sediment samples from the boundary layer that were investigated per site is given in Table 2. A duplicate polished section was

made from the sediments sample containing shocked quartz. All polished sections were inspected visually for the occurrence of PDFs in quartz using transmitted light microscopy (TLM).

After carbon coating, grains with planar microstructures were analyzed using scanning electron microscopy (SEM) cathodoluminescence (CL) imaging (see Hamers and Drury 2011) using a Philips XL30S FEG-SEM with a KE Developments Centaurus CL 8

Table 2. Information on the different Allerød-Younger Dryas boundary layers investigated.

Site name ^a	Type of boundary layer ^b	Nr. of samples investigated	Age ^c	Archaeology	Reported markers	Reference
Altdarss 39 (DE)	Peat layer	1	10,600 ± 55 ¹⁴ C yr BP ^d (12,660–12,540 cal. yr BP)			Kaiser et al. (2006)
Blankenforde (DE)	Finow soil	1	Between 15.5 ± 1 ka and 13.6 ± 0.6 ka ^e			Küster and Preusser (2009)
Dybowo (PL)	Finow soil	1	10,390 ± 50 ¹⁴ C yr BP (12,390–12,160 cal. yr BP)			This study; Kaiser et al. (2009)
Geldrop Aalsterhut (NL)	Usselo horizon ^d	3	10,845 ± 15 ¹⁴ C yr BP (12,740–12,710 cal. yr BP)	Federmesser, Ahrensburg	Nanodiamonds	Van Hoesel et al. (2012) Jankowski (2012)
Katarzynska (PL)	Usselo horizon and Finow soil	3	11,100 ± 270 ¹⁴ C yr BP ^e (13,195–12,725 cal. yr BP)			
Lommel Maatheide (BE)	Usselo horizon and peat layer	2	11,480 ± 100 ¹⁴ C yr BP (13,430–13,235 cal. yr BP); between 13.5 ± 0.9 ka and 11.3 ± 0.8 ka	Federmesser, Early Mesolithic	Nanodiamonds, iridium, magnetic spherules	Firestone et al. (2007); Tian et al. (2011); Derese et al. (2012); Wittke et al. (2013)
Lommel Molse Nete (BE)	Usselo horizon	1	11,480 ± 35 ¹⁴ C yr BP ^e (13,370–13,285 cal. yr BP)	Federmesser, Early Mesolithic		This study; Vanmontfort et al. (2011)
Lutterzand (NL)	Peat layer	3	10,480 ± 70 ¹⁴ C yr BP (12,560–12,240 cal. yr BP); between 13.8 ± 1.0 and 12.7 ± 0.9 ka			This study; Vandenbergh et al. (2013)
Murray Springs (USA)	Black Mat	2	10,885 ± 50 ¹⁴ C yr BP ^e (12,810–12,705 cal. yr BP)	Clovis	Nanodiamonds, iridium, magnetic spherules, glass-like carbon	Waters and Stafford (2007); Firestone et al. (2007); Kennett et al. (2009a); Haynes et al. (2010) Hilgers (2007)
Rosenberg (DE)	Finow soil	2	Between 15.71 ± 1.40 and 11.03 ± 1.20 ka ^e			

^aSee Fig. 1 for the locations of the site.^bSee Fig. 2 for photos of the sampled layers.^cOptical stimulated luminescence (OSL) ages are given in ka to show the difference in dating technique with the (calibrated) radiocarbon ages (given in ¹⁴C yr BP for the uncalibrated ages and cal. yr BP for the calibrated ages). Calendar (cal.) ages were calibrated using the IntCal13 calibration curve (Reimer et al. 2013) and the OxCalv4.2 calibration software (Bronk Ramsey 2009), and given within their 68.2% confidence interval.^dAt the Aalsterhut site, one sample from the coversands below was also investigated.^eAverage of multiple dates.

Table 3. AMS radiocarbon dates of individual charcoal particles from the palaeosol at different locations.

Sample name	Site	Sample nr. for AMS	^{14}C age BP	Cal. age BP ^a
Dyb-1	Dybowo	GrA-55464	10,390 ± 50	12,390–12,160
LZ-02	Lutterzand	GrA-55486	11,460 ± 50	13,380–13,255
LZB-01	Lutterzand	GrA-55616	10,930 ± 70	12,860–12,715
LZB-2	Lutterzand	GrA-55619	10,880 ± 50	12,785–12,710
LMN-01	Lommel Molse Nete	GrA-55466	11,050 ± 50	12,990–12,835
LMN-2	Lommel Molse Nete	GrA-55618	11,740 ± 110	13,710–13,465
LMN-3	Lommel Molse Nete	GrA-55621	11,930 ± 55	13,830–13,615

^aCalendar (cal.) ages were calibrated using the IntCal13 calibration curve (Reimer et al. 2013) and the OxCalv4.2 calibration software (Bronk Ramsey 2009), and given within their 68.2% confidence interval.

detector attached, which has a wavelength detection range of 300–650 nm with a peak at 420 nm. For some grains, additional SEM-CL images were taken using an FEI Nova Nanolab 600 SEM with a Gatan PanaCL detector, which is more or less panchromatic and has a detection range of 185–850 nm. Three images were taken with this detector, using a red (595–850 nm), green (495–575 nm), and blue (185–510 nm) filter and subsequently combined in a composite RGB image. In addition, on the XL30S FEG-SEM grains were analyzed using forescatter electron (FSE) imaging, also known as orientation contrast imaging, and electron backscatter diffraction (EBSD) mapping using an Oxford Instrument-HKL Channel 5 system equipped with a Nordlys CCD EBSD camera, with two FSE detectors attached in the lower corners of the camera. For this analysis samples were given an additional polish using 50 nm colloidal silica before carbon coating.

A thin foil for transmission electron microscopy (TEM) analysis was prepared using the FEI Nova Nanolab instrument and analyzed using a FEI Tecnai 20 FEG TEM operated at 200 kV. All electron microscopes are located at the Electron Microscopy Laboratory Utrecht (EMU).

For additional radiocarbon dating, charcoal particles from three sites (Table 3) were dated. After handpicking the mm-sized charcoal particles from the sand, the charcoal particles were treated following the standard acid-alkali-acid (AAA) method (Mook and Streurman 1983) to remove any adsorbed carbonates and soluble humic acids with ultrasonic cleaning during both acid steps. Radiocarbon ages were measured at the Groningen AMS facility (Van der Plicht et al. 2000).

RESULTS

The sediment fraction (20–250 µm) from the investigated boundary layers in the coversand area all contained >75 wt% quartz. The layers from the Netherlands as well as Katarzynka all consisted of 30 wt% of the lighter quartz fraction (D2.62–2.64 g cm⁻³) that was further investigated, the layers

from Blankenforde and Lommel contained a little more (37 wt%) of the lighter quartz fraction. The layer from Melchow differed from the others, in that the D2.62–2.64 g cm⁻³ fraction comprised 60 wt% of the total sediment fraction, probably because of a higher amount of feldspars. The two layers from Murray Springs contained more lighter minerals (44 wt% $D < 2.62$ g cm⁻³) compared to the European layers.

All polished sections (D2.62–2.64 g cm⁻³) contained quartz grains with tectonic deformation lamellae and fractures (Fig. 3) in various, small amounts as well as a small number of feldspar grains. Three quartz grains with multiple sets of lamellae were also observed (Figs. 3g–i and 4). The wavy nature of the lamellae of the first grain (Fig. 3g) clearly indicates that these are tectonic deformation lamellae (Drury 1993; Vernooij and Langenhorst 2005). The other two grains, although not convincing as PDFs in TLM (Figs. 4a and 4d), do show some features similar to PDFs in the SEM-CL images taken with the Centaurus detector (Figs. 3b and 3e). These features appear thin (<1–2 µm), closely spaced (<2 and 5–10 µm) and relatively straight. Color filtered CL imaging, on the other hand, shows that the features are relatively thick (8–15 µm) bands bound by thin, irregular red-luminescent lines and are thus not PDFs. In the sample from Lutterzand, a small grain containing one set of thin (<1–2 µm), closely spaced (<10 µm) lamellae was observed in TLM (Fig. 5a). As these lamellae were difficult to identify as twins using LM techniques, this grain was examined using SEM techniques. EDS spectra showed that the grain was feldspar: FSE imaging and EBSD further showed that the thin bands had different orientations consistent with twinning. Some of the boundaries are decorated by small pores. In the grayscale SEM-CL images, these feldspar twins closely resembled PDFs in quartz (Fig. 5).

One of the samples from the Usselo palaeosol at Geldrop Aalsterhut contained one relatively rounded quartz grain containing two sets of thin, closely spaced planar microfeatures in TLM (Fig. 6a) with a north–south and northeast–southwest orientation. When the microscope was focused slightly below the surface, a

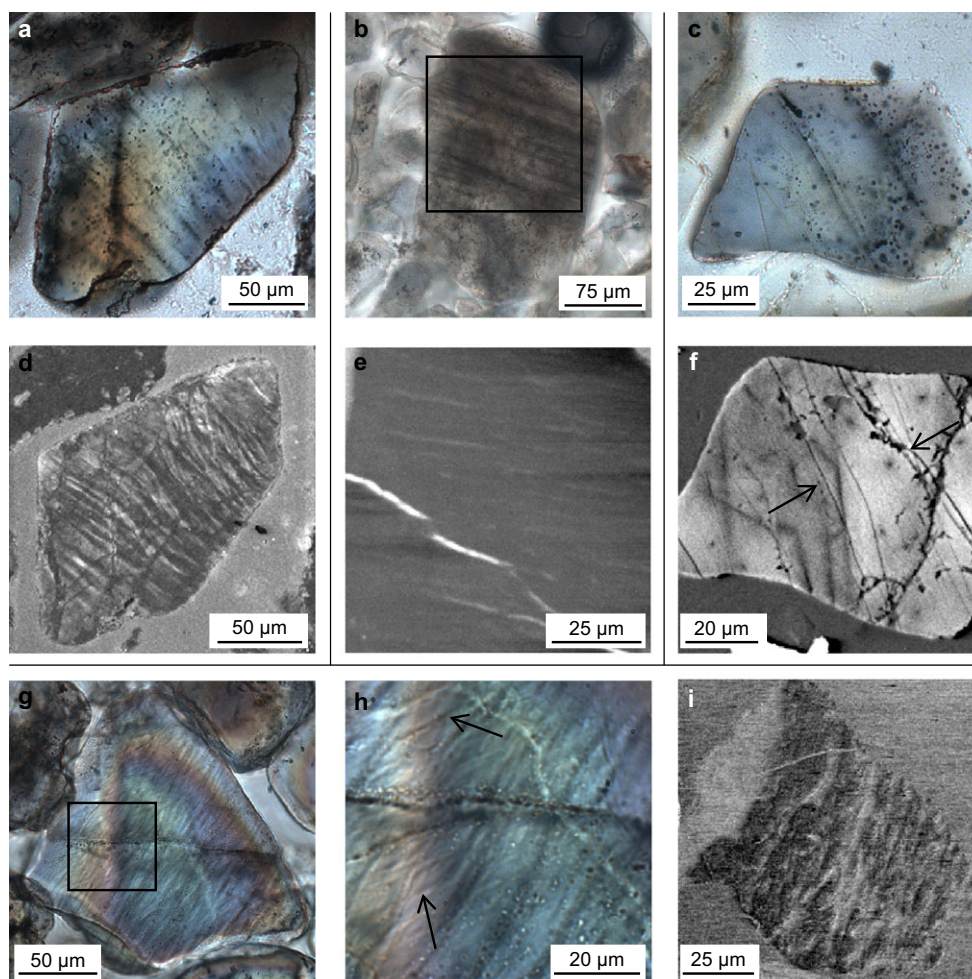


Fig. 3. Examples of polished surfaces of quartz grains with different kinds of (sub)planar microfeatures. a) Transmitted light microscopy (TLM) image of a grain with poorly defined subplanar microfeatures from the coversand underlying the Usselo palaeosol at Geldrop Aalsterhut. b) TLM image of a grain with relatively wide planar microstructures from the Usselo palaeosol at Geldrop Aalsterhut. c) TLM image of a grain with a few sharp (sub)planar microfeatures from the Finow palaeosol at Rosenberg. d) SEM-CL image of the grain in (a) showing microstructures characteristic of tectonic deformation lamellae. e) SEM-CL image of the grain in (b) (boxed region) showing weak contrast from tectonic deformation lamellae. f) SEM-CL image of the grain in (c) showing narrow, irregular nonluminescent features (arrows), possibly healed fractures. g) TLM image of a grain with closely spaced wavy tectonic deformation lamellae from the Usselo palaeosol at Lommel Maatheide. h) Higher magnification TLM image of the grain in (g) (boxed region) showing a second set of deformation lamellae (arrows). i) SEM-CL image of grain in (g) showing weak contrast from relatively wide features, compared to the narrow features visible in the TLM.

third set of lamellae was visible with a northwest–southeast orientation (Fig. 6b). SEM-CL imaging shows that the lamellae are mostly red luminescent and are sometimes lined by pores (Figs. 6c and 6d), suggesting that they are healed PDFs (Hamers 2013). A fourth set of lamellae (Fig. 6c, yellow arrow), not visible in TLM, can be seen in the bottom part of the grain and has a north–northeast to south–southwest orientation. No planar features with an orientation corresponding to the third set as seen in TLM (Fig. 6b) were seen in the SEM-CL images, suggesting that this set is only present in the part of the grain that is below the polished surface.

The pores along the lamellae are best visible in the FSE images (Fig. 7). The FSE images show trails of pores following the direction of the PDFs as well as two or three other orientations not seen in the TLM or SEM-CL image, one of these other orientations is visible in Fig. 7a, where they appear as a bright line or thin band. The EBSD pattern quality map (Fig. 7b) shows that the bright band in the FSE image has a less well ordered or amorphous crystal structure. Coesite and stishovite, which are denser phases of SiO_2 forms during high shock pressures, might also show up bright in the FSE image. These high pressure phases of SiO_2 would, however, show up brighter in the BSE image

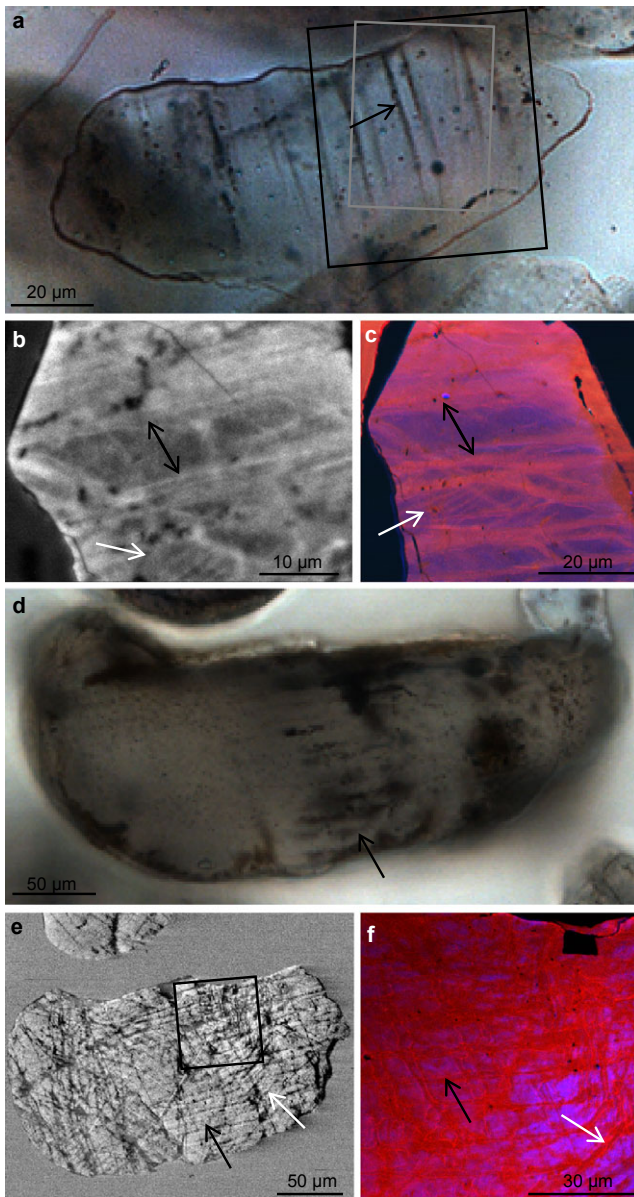


Fig. 4. Polished surfaces of quartz grains from the Usselo palaeosol at Geldrop Aalsterhut (a–c) and Katarzynka (d–f). TLM images (a, d) show (sub)planar microstructures that are not visible throughout the entire grain. Black and white SEM-CL images (b, e) of each grains show one set of thin, closely spaced microstructures that occur through most of the grain (black arrows) and a second set in some part of the grain (white arrows). Composite color CL images (c, f) however, show that these microstructures consist of slightly thicker bands bounded by thin, irregular red-luminescent lines. The gray and black boxes in (a) show the location of (b) and (c), respectively. Note that (b) and (c) are rotated counterclockwise compared to (a). The black box in (e) shows the location of (f).

compared to quartz (Stähle et al. 2008), while the features in our grain do not (Fig. 7c). The bright and variable contrast is consistent with that observed for healed PDFs (Hamers 2013).

The BSE image shows that the bright band in the FSE image is bounded by two converging boundaries, creating a narrow lens-shaped feature. Curved boundaries occur between the pores. The inverse pole figure map shows that the darker gray areas in the FSE and BSE image are Dauphiné twins (Fig. 7b). The boundaries of the twinned domains are often parallel to the planar microfeatures. Dauphiné twins are known to occur in shocked quartz, but their origin and relation to the PDFs is not completely understood (Trepmann and Spray 2005; French and Koeberl 2010; Hamers 2013).

Using FIB-SEM, a rectangular TEM foil was cut from the grain with its short side perpendicular to the grain surface and its long side perpendicular to one PDF set within the shocked quartz grain (see Figs. 6a and 7a for its location). TEM imaging of this thin foil shows the planar microfeatures as thin lines of high dislocation density (with an east-west orientation in Fig. 8). No amorphous phase, typical of fresh PDFs, was detected, suggesting that the features are healed PDFs. The orientation of the PDF traces is parallel to the short side of the TEM foil and thus perpendicular to the polished surface of the grain (imaged in TLM and SEM). Because the thin foil was sectioned perpendicular to the trace of the PDFs in the polished section (red box in Fig. 7a) the PDF boundaries in the TEM section (east-west in Fig. 8a) are approximately edge-on, that is, approximately perpendicular to the surface of the thin foil. Analysis of the TEM diffraction patterns (Fig. 8b) show that these PDFs are parallel to the $\{10\bar{1}4\}$ planes. Comparison of the 2-D traces of the PDFs to the pole figures based on the EBSD data indicates that the other two sets of planar microfeatures visible on the grain surface, are consistent with $\{10\bar{1}2\}$ and $\{10\bar{1}3\}$ planes. These orientations are common for PDFs in quartz (Ferrière et al. 2009). These PDFs were not sampled for TEM analysis or studied using the U-stage, therefore the orientation of these PDFs has not been confirmed. Although most PDFs are straight, TEM shows that some of the PDFs deviate toward the edge of the pores. When tilted off zone, areas of different brightness are seen in part of the grain, suggesting that these areas have a somewhat different crystal orientation. This difference in orientation also explains the slight streaking in the diffraction pattern (Fig. 8b).

The shocked quartz grain also contains several K-feldspar inclusions (10–20 µm in diameter), visible as dark particles in the SEM-CL image (Fig. 6c). SEM-BSE images show the presence of even smaller (up to 2 µm) inclusions in some of the pores that are aligned along the PDFs (best visible in the top of Fig. 7d). Due to the small size of the inclusions, the EDX spectra

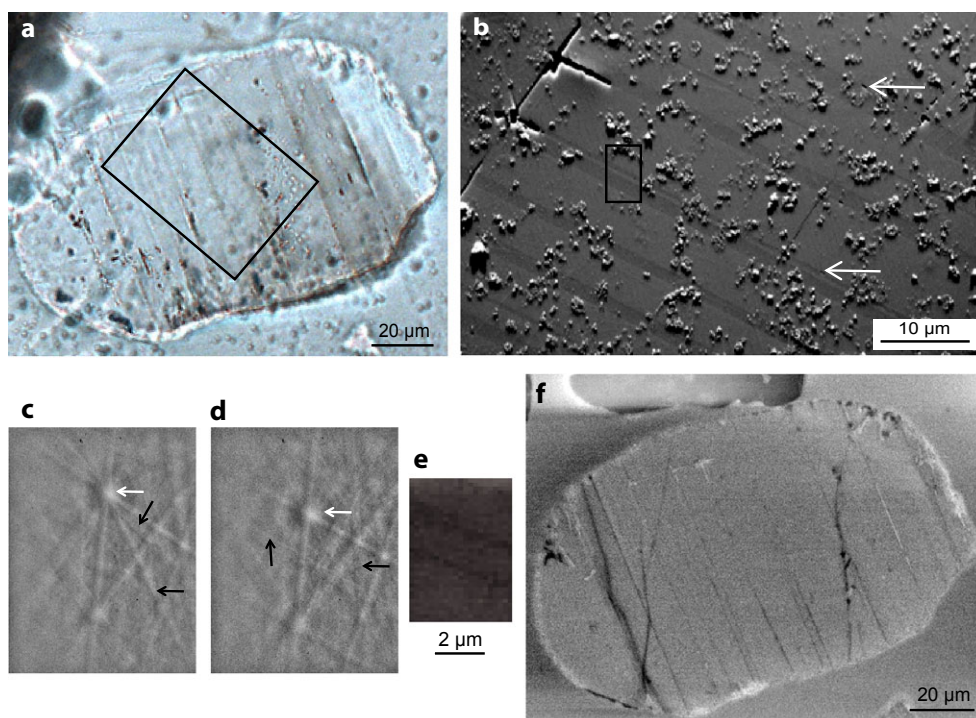


Fig. 5. Grain from the Usselo palaeosol at Lutterzand showing one set of thin, well-defined, closely spaced planar thin lamellae that cross the entire grain in plain polarized light (a). EDS spectra showed that the grain was feldspar. b) FSE image of the boxed region in (a) showing dark-gray bands of varying thickness with a different orientation than the matrix (light gray). Small pores are visible (arrows) along some boundaries. EBSD patterns of the dark bands (c) and the matrix (d) show a shift of one of the poles (white arrow) and changes in the bands that are visible (some indicated with black arrows). Patterns are rotated 90° clockwise. e) EBSD pattern quality map of the boxed region in (b) shows thin lines of lower pattern quality, which occur at the boundaries between the two crystal orientations. These regions might correspond to the thin features in the SEM-CL image (f), which shows that the twins are nonluminescent.

include information of the surrounding quartz. The inclusions generally contain sulfur, often in combination with the presence of iron or titanium (Fig. 7e). Inclusions with only iron or sulfur in combination with calcium were also observed.

No other shocked quartz grains were observed in the polished section containing the shocked quartz grain, a duplicate polished section made from the same sample, or the polished sections from different samples from the same site.

DISCUSSION

Identification of Planar Deformation Features

Tectonic deformation lamellae are often easily distinguishable from PDFs in light microscopy (e.g., Fig. 3a), especially when only one set is observed. However, although the occurrence of multiple sets of (sub)planar features is often seen as typical of PDFs (Table 1), several nonshocked grains with more than one set of subplanar features were observed

(Figs. 3g–i and 4). In addition, sometimes we observed tectonic deformation lamellae that were visible as one set of relatively well-defined, parallel features (e.g., Fig. 3b), which might be confused with PDFs in light microscopy by an inexperienced user. Using SEM-CL images (e.g., Figs. 3d and 3e) these tectonic deformation lamellae were easily distinguishable from PDFs, as PDFs are sharp and well-defined in SEM-CL imaging, whereas tectonic deformation lamellae are not (Hamers and Drury 2011). For identifying the nature of the features in Fig. 4, color filtered CL imaging proved to be better in distinguishing between PDFs and other features than the limited wavelength of grayscale CL imaging. Universal stage measurements may be used to distinguish between the 3D crystallographic orientation of this kind of ambiguous features and PDFs (Stöffler and Langenhorst 1994; Ferrière et al. 2009), but our samples were rather thick for U-stage analysis. Although TLM of polished sections gives a good indication for the occurrence of PDFs, other techniques, such as SEM-CL imaging (preferably color filtered), universal stage measurements, and/or TEM analysis are

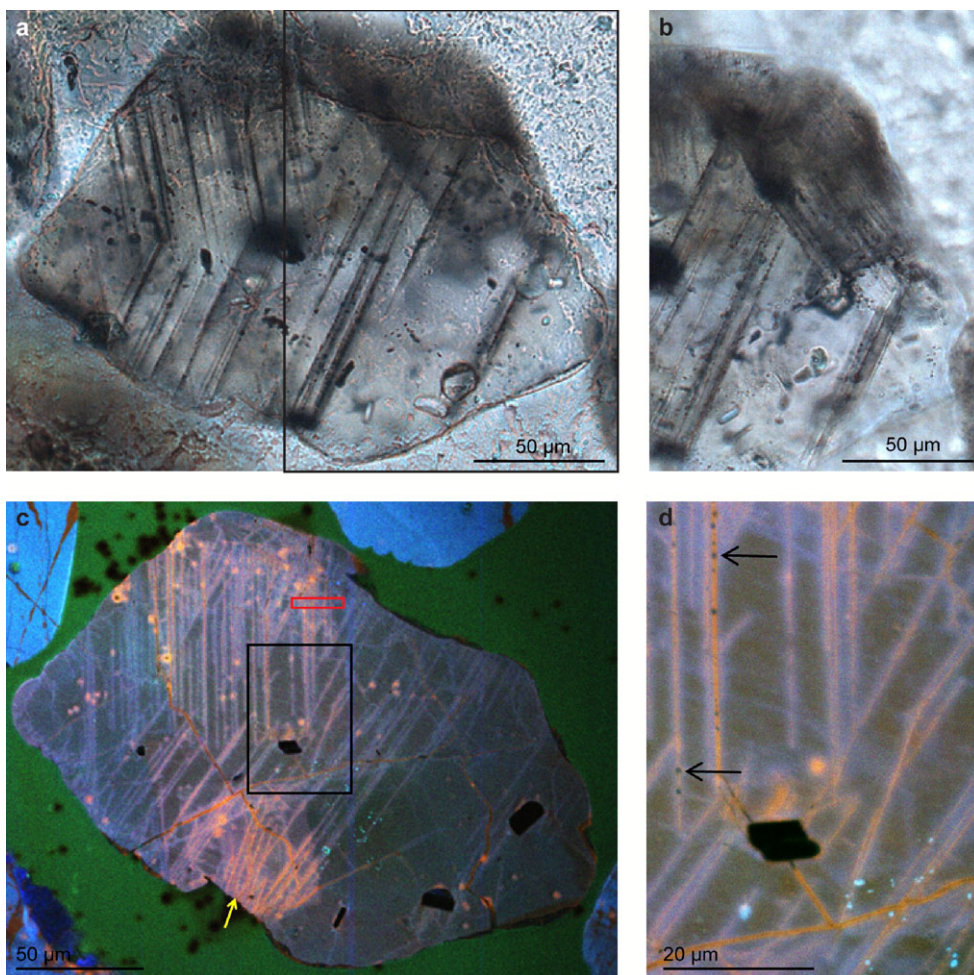


Fig. 6. Quartz grain containing PDFs from the Usselo palaeosol at Geldrop Aalsterhut. a) TLM image showing two sets of thin, closely spaced planar microfeatures. b) A third set of planar microfeatures is visible slightly below the surface of the polished section. c) Composite color CL-image of the grain showing that the microfeatures are mostly red-luminescent. A fourth orientation is visible in the bottom part of the grain. The black features are small feldspar inclusions. Red rectangle indicates the location of the TEM foil. The north-south oriented PDFs are parallel. d) Higher magnification composite color CL-image showing some pores or fluid inclusions (arrows) along the PDFs. The irregular orange-luminescent feature is probably a healed fracture.

thus necessary to convincingly identify PDFs (e.g., Ferrière et al. 2009; French and Koeberl 2010; Hamers and Drury 2011). Analysis of the topography of the outer surface of a grain using SEM, as carried out by Mahaney et al. (2010a), cannot be used to convincingly identify PDFs (French and Koeberl 2010). Our results also indicate that for a feldspar, where grains may contain thin ($<2 \mu\text{m}$) twins decorated by inclusions, differentiating the twins from PDFs in quartz may be difficult when no other microstructural features such as cleavage, zoning, or alteration are visible. EDS or a more complete microstructural analysis might thus be necessary in the uncommon situation that no discrimination can be made using TLM. Thicker twins in feldspars should be easily identified in cross polarized TLM.

Origin of the Shocked Quartz Grain

Among the quartz grains we studied from 20 samples (roughly 1500 grains per sample) in 11 Lateglacial palaeosol and peat layers containing the Allerød-Younger Dryas transition (see Table 2), only one shocked quartz grain was found: this grain was found in one of the samples taken from the Geldrop Aalsterhut site. A duplicate polished section from the same sample did not contain any shocked grains and neither did the sections from the other two samples from the same layer. The absence of any shocked grains in a duplicate section from the same sample and in sections from other samples from the Usselo palaeosol from the same and nearby sites (Lommel) implies that either the concentration of shocked grains is very low or

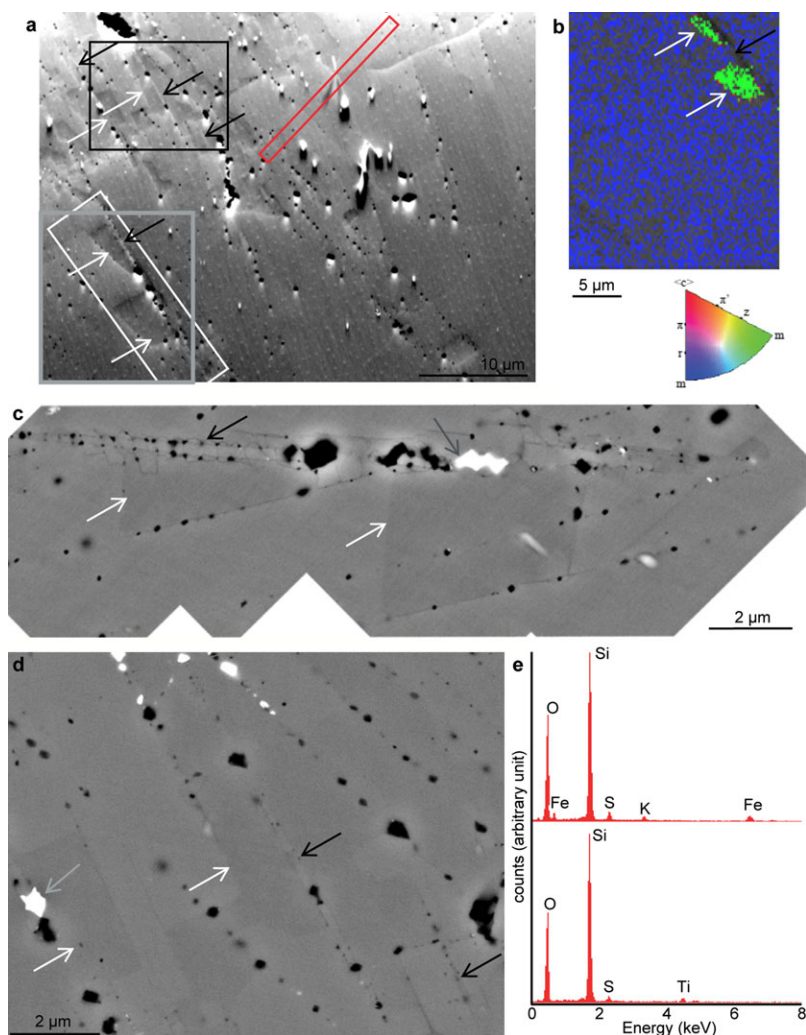


Fig. 7. a) FSE image of part of the quartz grain shown in Fig. 6 clearly showing the planar microfeatures as trails of pores in multiple orientations. Darker and lighter gray areas, partly bound by the PDFs, are visible. At some locations a thin bright band is visible along the planar microfeatures (black arrows). Red rectangle indicates the location of where the TEM foil was created. White arrows show Dauphiné twins; gray box is shown in (b), white box in (c), and black box in (d). b) Pattern quality map and inverse pole figure map of the gray box in (a) showing that the dark areas in (a) are Dauphiné twins (white arrows) and that the planar microfeature is characterized by lower pattern quality (the feature is visible as a dark line) and thus a less well organized or possibly amorphous crystal structure (black arrow). The EBSD map has been distorted as a result of charging and was digitally stretched to match the geometry of the FS image. c) BSE image of the two Dauphiné twins (white arrows) and the bright planar microfeature in the white box in (a). The Dauphiné twins are visible as blocky darker areas. The band corresponding to the bright planar microfeature in the FSE image is bounded by two lines of pores (black arrow) that converge toward each other near the edge of the image. The pores in each line are connected by small curved lines, which are possibly thin cracks. The bright white feature (gray arrow) is an inclusion containing iron. d) BSE image of the area in the black rectangle in (a), showing the Dauphiné twin boundaries (white arrows). The bright features in the FSE image (black arrows) are again visible as two lines that converge toward each other in both directions. e) EDX spectra of two of the bright inclusions in BSE images that occur in the pores aligning the PDFs (gray arrows in c and d). The top spectrum shows the composition of the S-, Fe-, and K-rich inclusion in (c). The bottom spectrum shows the composition of the largest inclusion in (d), which is Ti- and S-rich. Because of their small size, the EDX spectra are dominated by the X-rays of the surrounding quartz.

that one sample was contaminated. Based on a rough estimate of the number of grains investigated from the Usselo horizon at Aalsterhut (~6000) and the presence of only one shocked grain, it is expected that the coversand contains <0.02% of shocked quartz grains.

Alternatively, contamination is possible, as samples were embedded and polished in a laboratory where other shocked quartz samples were processed. Although all preparation equipment was thoroughly cleaned between samples, there is a chance that the grain

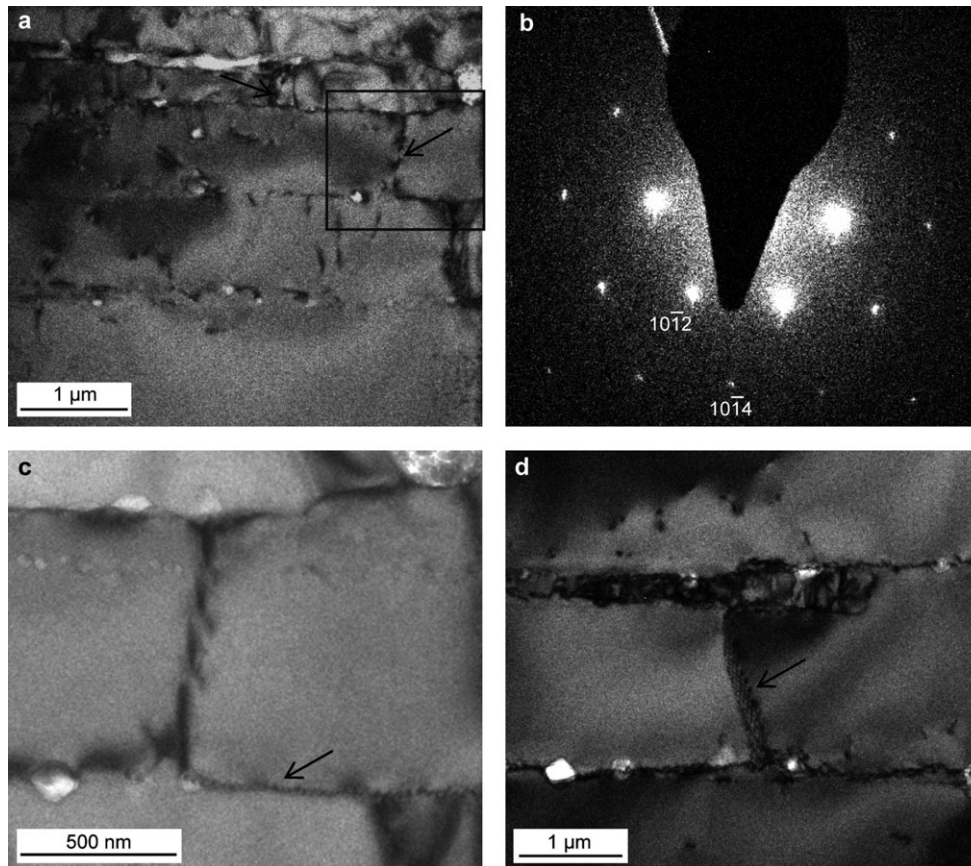


Fig. 8. TEM images of the FIB prepared TEM thin foil that was sectioned perpendicular to the trace of one of the PDF sets in the grain, see Figs. 6c and 7a (red rectangle). The right- and left-hand sides in the TEM image are parallel to the polished grain surface. a) TEM BF image detail of part of the top of the thin foil (corresponding to the bottom left corner of the red rectangle in Figs. 6a and 7c). Traces of the PDFs (east–west in the image) are approximately edge-on and parallel to the $\{10\bar{1}4\}$ planes as shown in the corresponding diffraction pattern in (b). Features perpendicular to the PDFs (north–south orientation, see arrows) are also observed and might be twin boundaries. c) Higher resolution image of part of the thin foil tilted slightly off zone, showing that the PDFs consist of lines of dislocations (arrow). d) TEM BF image of a different part of the thin foil, at a different tilt, showing a dislocation network (arrow) between two PDFs.

originated from cross contamination from another sample. However, the concentration of shocked quartz grains in samples from known impact craters was also low so the chance of contamination is extremely small. Below we discuss other possible origins of the shocked grain.

There are several questions when attempting to relate the shocked quartz grain from Aalsterhut to the Younger Dryas impact event. According to an early version of the Younger Dryas impact hypothesis (Firestone et al. 2007), multiple objects exploded above or hit the Laurentide ice sheet in North America. If we assume that these objects penetrated the ice or also hit the unglaciated surface, shocked quartz could have been formed, ejected into the atmosphere, and subsequently have been incorporated in the Allerød-Younger Dryas boundary layer. The shocked grain found in the Usselo palaeosol in this study is, however, relatively large

($\sim 200 \times 150 \mu\text{m}$) compared to, for example, the average size of shocked quartz grains found in the K/T boundary in Europe ($\sim 100 \mu\text{m}$; Morgan et al. 2006). This relatively large size grain makes it unlikely that the grain is related to an event in North America involving much smaller impactors, as suggested by Firestone et al. (2007).

In a more recent version of the Younger Dryas impact hypothesis, however, an event consisting of multiple airbursts occurring around the globe is presented (Bunch et al. 2012), rather than possible impacts in North America. Although shocked quartz is not formed in airbursts, one could hypothesize that one of the objects entering the Earth's atmosphere did not explode in an airburst but actually hit the ground, forming a small crater of only a few meters in diameter. Such a small crater would have easily been eroded or filled in by aeolian activity during the Younger Dryas

or the Holocene. A small, local impact might also explain the occurrence of nanodiamond at the site (Van Hoesel et al. 2012). However, no disturbances in the Usselo palaeosol, indicative of a small local impact, have been found at the Geldrop Aalsterhut site, although these could have been present at the nonexcavated parts of the site.

Most importantly, although the Usselo palaeosol in which the shocked grain was found forms a visible boundary between the Younger Dryas coversand and the older sediments, this palaeosol was formed in older sediments present at the surface during most of the Allerød and the early Younger Dryas (at least for several centuries). So, although the Allerød-Younger Dryas boundary was sampled, in the form of the Usselo palaeosol, relating the single grain in the Usselo horizon to the proposed age of the Younger Dryas impact event with certainty would thus be difficult because the grain could have been incorporated into the Usselo palaeosol anytime during the palaeosol formation, and not necessarily at the onset of the Younger Dryas. If it is assumed that the nanodiamond found in glass-like carbon from the Usselo palaeosol at the same site (Van Hoesel et al. 2012) was also formed during an impact, and if the nanodiamond can be related to the charcoal in the same layer, the shocked quartz grain might also be dated to $10,845 \pm 15$ ^{14}C yr BP ($n = 14$; Van Hoesel et al. 2012) or 12,740–12,710 cal. yr BP (IntCal13). Nanodiamonds in distal ejecta layers are, however, not considered diagnostic evidence for an extraterrestrial impact event and might have a different origin (French and Koeberl 2010; Glass and Simonson 2012; Reimold and Jourdan 2012). Assuming a small local impact, it is also possible that this event occurred prior to the formation of the Usselo palaeosol and was incorporated into the coversand at an earlier stage, in which case the grain could be hundreds to thousands of years older. Although more shocked grains might be expected to have formed, they could have easily been dispersed by aeolian activity.

One way to assess whether the shocked quartz found in the Usselo palaeosol might have formed recently is to identify amorphous PDFs, as these only occur in relatively young impact material (e.g., French and Koeberl 2010). The PDFs in the grain are, however, aligned with pores or fluid inclusions, are red-luminescent, and consist of dislocation arrays rather than amorphous material, which suggest that the PDFs are healed and the grain thus experienced postimpact alteration (Stöffler and Langenhorst 1994; Trepmann and Spray 2006; Hamers 2013). Although healing can occur immediately following the impact, healed PDFs are most common in older impact material (i.e., several

million years) (Grieve et al. 1996; French and Koeberl 2010). This suggests that the shocked grain might be older than the Late-Glacial period. Shocked quartz grains can be eroded from older craters or distal ejecta layers and incorporated into the sediment (Cavosie et al. 2010) and the rounded shape of the grain suggests that it has been transported either prior to, or after impact. There are several possible older impact layers from which the grain might originate. The coversand in the Netherlands is mostly of local sedimentary origin (Crommelin 1964), which, in the southern Netherlands consist of older fluvial deposits from the Meuse river system. The K/T boundary (65 Ma) has been found in the Meuse catchment (Smit and Brinkhuis 1996), although no shocked quartz was found (Hamers 2013) and shocked quartz grain sizes found in the K/T boundary in Europe are usually smaller than the grain we found (Morgan et al. 2006). The Ries and Steinheim craters in southern Germany (15 Ma) are located in close proximity to the (current) catchment of the river Rhine, which could have transported material from the ejecta layer to the Netherlands. There are also several craters in Scandinavia, which might be the source of the shocked quartz grain as the glacial ice could have eroded the craters and transported the material south. It is, however, unlikely that this material reached the southern Netherlands as the glacial ice and its meltwater never reached this part of the country, although a small amount of material could have been transported by aeolian activity. Alternatively, the grain could be related to a pre-Late Glacial small scale impact, after which the small crater would have been eroded and the shocked sediment dispersed in the coversand.

Similar to the S-, Fe-, and Ti- rich inclusions found along the PDFs in our grain, magnetite inclusions along PDFs have also been observed in shocked quartz from the Vredefort crater (Cloete et al. 1999; Hart et al. 2000). In addition, experiments have shown that during an impact, shocked quartz might become enriched in material from the impactor (Ebert et al. 2013; note that no inclusions were reported). The presence of these inclusions could thus be related to the impact.

In summary, in our TLM study of the quartz fraction of the Usselo palaeosol from multiple sites in Europe and the Black Mat in North America, we found several grains that showed features somewhat similar to those of shocked quartz. However, SEM imaging shows that only one of these grains contains PDFs indicative of a shock event. This grain came from the Usselo palaeosol at Geldrop Aalsterhut, where nanodiamond of early Younger Dryas age has been found (Van Hoesel et al. 2012). Although the shocked grain was found in the Usselo palaeosol,

which was at the surface during the onset of the Younger Dryas, the healed nature of the PDFs suggests that the grain is probably older. Because only one grain was found at only one of the sites, we suggest that the shocked grain might have been eroded from an older impact layer and transported to the southern Netherlands, where it was eventually incorporated in the coversand in which the Usselo palaeosol was formed. Alternatively, assuming that the shocked grain was found in situ, the grain could have been deposited in the Usselo palaeosol at any point in time during its formation period (14,000–12,000 yr ago) and not just at the Younger Dryas onset. Further studies searching for shocked quartz and other impact markers in the Allerød-Younger Dryas boundary at nearby sites with better dating resolution, would be necessary before the shocked quartz grain at Geldrop Aalsterhut could be used to support a Late-Glacial impact event. Failure to find shocked quartz, however, does not necessarily invalidate the Younger Dryas impact hypothesis as airbursts are not likely to result in the necessary shock pressures at the surface.

CONCLUSIONS

Among the eleven palaeosol and peat layers of approximate Allerød-Younger Dryas age, only one shocked quartz grain was found, namely in the Usselo palaeosol at Geldrop Aalsterhut. Assuming that the grain was found in situ, the grain could have been deposited in the Usselo palaeosol at any point in time during its formation period (14,000–12,000 yr ago), and not just at the time of the proposed Younger Dryas impact event. However, considering that only one grain was found and assuming no contamination of the sample, we suggest that the grain was not found in situ, but most likely eroded from an older impact layer and incorporated in the coversand in which the palaeosol was formed. Although the PDFs in the grain should have been formed during an extraterrestrial impact, if it occurred, a single shocked quartz grain cannot be unequivocally used to support the Younger Dryas impact hypothesis.

Acknowledgments—Jos Deeben, Bart van Montfoort, Jan Willem de Kort, Kees Kasse, and Yvonne A'Campo are greatly acknowledged for their assistance with the fieldwork. Roel van Elsas is acknowledged for his great help with the density separation, Otto Stiekema, and Wynanda Koot for polishing the grains. Hans Meeldijk and Chris Schneijdenberg are thanked for their help with the electron microscopes. Radiocarbon ages were measured by the Groningen AMS facility. We also like to thank Carl Alwmark,

Ludovic Ferrière, and Michael Poelchau for their helpful comments. The contributions of Knut Kaiser and Mathias Küster were enabled by the projects ICLEA and TERENO of the Helmholtz Association.

Editorial Handling—Dr. Michael Poelchau

REFERENCES

- Alwmark C. 2009. Shocked quartz grains in the polymict breccia of the Granby structure, Sweden—Verification of an impact. *Meteoritics & Planetary Science* 44:1107–1113.
- Bohor B. F., Modreski P. J., and Foord E. E. 1987. Shocked quartz in the Cretaceous-Tertiary boundary clays: Evidence for a global distribution. *Science* 236:705–708.
- Bronk Ramsey C. 2009. Bayesian analysis of radiocarbon dates. *Radiocarbon* 51:337–360.
- Bunch T. E., Hermes R. E., Moore A. M. T., Kennett D. J., Weaver J. C., Wittke J. H., DeCarli P. S., Bischoff J. L., Hillman G. C., Howard G. A., Kimbel D. R., Kletetschka G., Lipo C. P., Sakai S., Revay Z., West A., Firestone R. B., and Kennett J. P. 2012. Very high-temperature impact melt products as evidence for cosmic airbursts and impacts 12,900 years ago. *Proceedings of the National Academy of Sciences* 109:1903–1912.
- Cavosie A. J., Quintero R. R., Radovan H. A., and Moser D. E. 2010. A record of ancient cataclysm in modern sand: Shock microstructures in detrital minerals from the Vaal River, Vredefort Dome, South Africa. *Geological Society of America Bulletin* 122:1968–1980.
- Cloete M., Hart R. J., Schmid H. K., Drury M., Demanet C. M., and Sankar K. V. 1999. Characterization of magnetite particles in shocked quartz by means of electron- and magnetic force microscopy: Vredefort, South Africa. *Contributions to Mineralogy and Petrology* 137:232–245.
- Crommelin R. D. 1964. A contribution to the sedimentary petrology and provenance of young Pleistocene cover sand in the Netherlands. *Geologie en Mijnbouw* 43:389–402.
- Derese C., Vandenberghe D. A. G., Van Gils M., Mees F., Paulissen E., and van den Haute P. 2012. Final Palaeolithic settlements of the Campine region (NE Belgium) in their environmental context: Optical age constraints. *Quaternary International* 251:7–21.
- Drury M. 1993. Deformation lamellae in metals and minerals. Defects and processes in the solid state: Geoscience applications. *The McLaren Volume, Developments in Petrology* 14:195–212.
- Ebert M., Hecht L., Deutsch A., and Kenkmann T. 2013. Chemical modification of projectile residues and target material in a MEMIN cratering experiment. *Meteoritics & Planetary Science* 48:134–149.
- Ferrière L., Morrow J. R., Amgaa T., and Koeberl C. 2009. Systematic study of universal-stage measurements of planar deformation features in shocked quartz: Implications for statistical significance and representation of results. *Meteoritics & Planetary Science* 44:925–940.
- Firestone R. B., West A., Kennett J. P., Becker L., Bunch T. E., Revay Z. S., Schultz P. H., Belgia T., Kennett D. J., Erlandson J. M., Dickenson O. J., Goodyear A. C., Harris R. S., Howard G. A., Kloosterman J. B., Lechler P., Mayewski P. A., Montgomery J., Poreda R., Darrah T., Que Hee S. S., Smith A. R., Stich A., Topping W., Wittke J. H., and Wolbach W. S. 2007. Evidence for an extraterrestrial

- impact 12,900 years ago that contributed to the megafaunal extinctions and the Younger Dryas cooling. *Proceedings of the National Academy of Sciences* 104:16,016–16,021.
- French B. M. 1998. Traces of Catastrophe: A Handbook of Shock-metamorphic Effects in Terrestrial Meteorite Impact Structures. LPI Contribution 954. Houston, Texas: Lunar and Planetary Institute. 120 p.
- French B. M. and Koeberl C. 2010. The convincing identification of terrestrial meteorite impact structures: What works, what doesn't, and why. *Earth-Science Reviews* 98:123–170.
- Glass B. P. and Simonson B. M. 2012. Distal impact ejecta layers: Spherules and more. *Elements* 8:43–48.
- Goltrant O., Cordier P., and Doukhan J.-C. 1991. Planar deformation features in shocked quartz; a transmission electron microscopy investigation. *Earth and Planetary Science Letters* 106:103–115.
- Grieve R. A. F., Langenhorst F., and Stöffler D. 1996. Shock metamorphism of quartz in nature and experiment: II. Significance in geoscience. *Meteoritics & Planetary Science* 31:6–35.
- Hamers M. F. 2013. Identifying shock microstructures in quartz from terrestrial impacts: New scanning electron microscopy methods. *Utrecht Studies in Earth Sciences* 32:191.
- Hamers M. F. and Drury M. R. 2011. Scanning electron microscope-cathodoluminescence (SEM-CL) imaging of planar deformation features and tectonic deformation lamellae in quartz. *Meteoritics & Planetary Science* 46:1814–1831.
- Hart R., Connell S., Cloete M., Mare L., Drury M., and Tredoux M. 2000. “Super magnetic” rocks generated by shock metamorphism from the centre of the Vredefort impact structure, South Africa. *South African Journal of Geology* 103:151–155.
- Haynes C. V. Jr. 2008. Younger Dryas “black mats” and the Rancholabrean termination in North America. *Proceedings of the National Academy of Sciences* 105:6520–6525.
- Haynes C. V., Boerner J., Domanik K., Laretta D., Ballenger J., and Goreva J. 2010. The Murray Springs Clovis site, Pleistocene extinction, and the question of extraterrestrial impact. *Proceedings of the National Academy of Sciences* 107:4010–4015.
- Hijzeler C. C. W. J. 1947. De oudheidkundige opgravingen in Twente in de laatste jaren. In *Een kwart eeuw oudheidkundig bodemonderzoek in Nederland*, edited by van Gelder H. E., Glazema P., and Bontekoe G. A. Meppel, the Netherlands: Boom & Zoom. pp. 327–349.
- Hilgers A. 2007. The chronology of Late Glacial and Holocene dune development in the northern Central European lowland reconstructed by optically stimulated luminescence (OSL) dating. Ph.D. thesis, University of Cologne, 440 p.
- Holm S., Alwmark C., Alvarez W., and Schmitz B. 2011. Shock barometry of the Siljan impact structure, Sweden. *Meteoritics & Planetary Science* 46:1888–1909.
- Jankowski M. 2012. Lateglacial soil paleocatena in inland-dune area of the Toruń Basin, Northern Poland. *Quaternary International* 265:116–125.
- Kaiser K., Barthelmes A., Czakó Pap S., Hilgers A., Janke W., Kühn P., and Theuerkauf M. 2006. A Lateglacial palaeosol cover in the Altdarss area, southern Baltic Sea coast (northeast Germany): Investigations on pedology geochronology and botany. *Geologie en Mijnbouw/Netherlands Journal of Geosciences* 85:197–220.
- Kaiser K., Hilgers A., Schlaak N., Jankowski M., Kühn P., Bussemer S., and Przegietka K. 2009. Palaeopedological marker horizons in northern central Europe: Characteristics of Lateglacial Usselo and Finow soils. *Boreas* 38:591–609.
- Kasse C. 2002. Sandy aeolian deposits and environments and their relation to climate during the Last Glacial Maximum and Lateglacial in northwest and central. *Europe Progress in Physical Geography* 26:507–532.
- Kennett D. J., Kennett J. P., West A., Mercer C., Que Hee S. S., Bement L., Bunch T. E., Sellers M., and Wolbach W. S. 2009a. Nanodiamonds in the Younger Dryas boundary sediment layer. *Science* 323:94.
- Kennett D. J., Kennett J. P., West A., West G. J., Bunch T. E., Culletona B. J., Erlandson J. M., Que Hee S. S., Johnson J. R., Mercer C., Shen F., Sellers M., Stafford T. W. Jr, Stich A., Weaver J. C., Wittke J. H., and Wolbach W. S. 2009b. Shock-synthesized hexagonal diamonds in Younger Dryas boundary sediments. *Proceedings of the National Academy of Sciences* 106:12,623–12,628.
- Küster M. and Preusser F. 2009. Late Glacial and Holocene aeolian sands and soil formation from the Pomeranian outwash plain (Mecklenburg, NE-Germany). *E&G Quaternary Science Journal* 58:156–163.
- Langenhorst F. 2002. Shock metamorphism of some minerals: Basic introduction and microstructural observations. *Vestnik Ceskeho Geologickeho Ustavu* 77:265–282.
- Langenhorst F. and Deutsch A. 2012. Shock metamorphism of minerals. *Elements* 8:31–36.
- Leroux H. and Doukhan J.-C. 1996. A transmission electron microscope study of shocked quartz from the Manson impact structure. In *The Manson impact structure, Iowa: Anatomy of an impact crater*, edited by Koeberl C. and Anderson R. R. GSA Special Paper 302. Boulder, Colorado: Geological Society of America. pp. 267–274.
- Mahaney W. C., Kalm V., Krinsley D. H., Tricart P., Schwartz S., Dohm J., Kim K. J., Kapran B., Milner M. W., Beukens R., Boccia S., Hancock R. G. V., Hart K. M., and Kelleher B. 2010a. Evidence from the northwestern Venezuelan Andes for extraterrestrial impact: The black mat enigma. *Geomorphology* 116:48–57.
- Mahaney W. C., Krinsley D., and Kalm V. 2010b. Evidence for a cosmogenic origin of fired glaciofluvial beds in the northwestern Andes: Correlation with experimentally heated quartz and feldspar. *Sedimentary Geology* 231:31–40.
- Meltzer D. J., Holliday V. T., Cannon M. D., and Miller D. S. 2014. Chronological evidence fails to support claim of anisochronous widespread layer of cosmic impact indicators dated to 12,800 years ago. *Proceedings of the National Academy of Sciences* 111:E2162–E2171.
- Mook W. G. and Streurman H. J. 1983. Physical and chemical aspects of radiocarbon dating. *Pact Publications* 8:31–55.
- Morgan J., Lana C., Kearsley A., Coles B., Belcher C., Montanari S., Díaz-Martínez E., Barbosa A., and Neumann V. 2006. Analyses of shocked quartz at the global K-P boundary indicate an origin from a single, high-angle, oblique impact at Chicxulub. *Earth and Planetary Science Letters* 251:264–279.
- Petaev M. I., Huang S., Jacobsen S. B., and Zindler A. 2013. Large Pt anomaly in the Greenland ice core points to a cataclysm at the onset of Younger Dryas. *Proceedings of the National Academy of Sciences* 110:12,917–12,920.

- Pinter N., Scott A. C., Daulton T. L., Podoll A., Koeberl C., Anderson R. S., and Ishman S. E. 2011. The Younger Dryas impact hypothesis: A requiem. *Earth-Science Reviews* 106:247–264.
- Reimer P. J., Bard E., Bayliss A., Beck J. W., Blackwell P. G., Bronk Ramsey C., Grootes P. M., Guilderson T. P., Hafliðason H., Hajdas I., Hatté C., Heaton T. J., Hoffmann D. L., Hogg A. G., Hughen K. A., Kaiser K. F., Kromer B., Manning S. W., Niu M., Reimer R. W., Richards D. A., Scott E. M., Southon J. R., Staff R. A., Turney C. S. M., and van der Plicht J. 2013. IntCal13 and Marine13 radiocarbon age calibration Curves 0–50,000 Years cal BP. *Radiocarbon* 55:1869–1887.
- Reimold W. U. and Jourdan F. 2012. Impact!—Bolides, craters, and catastrophes. *Elements* 8:19–24.
- Reimold W. U., Ferrière L., Deutsch A., and Koeberl C. 2014. Impact controversies: Impact recognition criteria and related issues. *Meteoritics & Planetary Science* 49:723–731.
- Schlaak N. 1993. Studie zur Landschaftsgenese im Raum Nordbarnim und Eberswalder Urstromtal. *Berliner Geographische Arbeiten* 76:145.
- Smit J. and Brinkhuis H. 1996. The Geulhemmerberg Cretaceous/Tertiary boundary section (Maastrichtian type area, SE Netherlands); summary of results and a scenario of events. *Geologie en Mijnbouw* 75:283–293.
- Stähle V., Altherr R., Koch M., and Nasdala L. 2008. Shock-induced growth and metastability of stishovite and coesite in lithic clasts from suevite of the Ries impact crater (Germany). *Contributions to Mineralogy and Petrology* 155:457–472.
- Stöffler D. and Langenhorst F. 1994. Shock metamorphism of quartz in nature and experiment: I. Basic observation and theory. *Meteoritics* 29:155–181.
- Tian H., Schryvers D., and Claeys P. 2011. Nanodiamonds do not provide unique evidence for a Younger Dryas impact. *Proceedings of the National Academy of Sciences* 108:40–44.
- Trepmann C. A. and Spray J. G. 2005. Planar microstructures and Dauphiné twins in shocked quartz from the Charlevoix impact structure, Canada. *Geological Society of America Special Papers* 384:315–328.
- Trepmann C. A. and Spray J. G. 2006. Shock-induced crystal-plastic deformation and post-shock annealing of quartz microstructural evidence from crystalline target rocks of the Charlevoix impact structure, Canada. *European Journal of Mineralogy* 18:161–173.
- Van der Plicht J., Wijma A., Aerts A. T., Pertuisot M. H. P., and Meijer H. A. J. 2000. The Groningen AMS facility: Status report. *Nuclear Instruments and Methods in Physics Research B* 172:58–65.
- Van Hoesel A., Hoek W. Z., Braadbaart F., van der Plicht J., Pennock G. M., and Drury M. R. 2012. Nanodiamonds and wildfire evidence in the Usselo horizon postdate the Allerød-Younger Dryas boundary. *Proceedings of the National Academy of Sciences* 109:7648–7653.
- Van Hoesel A., Hoek W. Z., Pennock G. M., and Drury M. R. 2014. The Younger Dryas impact hypothesis: A critical review. *Quaternary Science Reviews* 83:95–114.
- Vandenberghé D. A. G., Derese C., Kasse C., and Van den Haute P. 2013. Late Weichselian (fluvio-)aeolian sediments and Holocene drift-sands of the classic type locality in Twente (E Netherlands): A high-resolution dating study using optically stimulated luminescence. *Quaternary Science Reviews* 68:96–113.
- Vanmontfort B., Yperman W., Lambrechts B., van Gils M., and Geerts F. 2011. Een finaalpaleolithisch en mesolithisch sitecomplex the Lommel, Molste Nete. Opggravingscampagne 2010. *Notae Praehistoricae* 30:29–34.
- Vernooij M. G. C. and Langenhorst F. 2005. Experimental reproduction of tectonic deformation lamellae in quartz and comparison to shock-induced planar deformation features (abstract). *Meteoritics & Planetary Science* 40:1353–1361.
- Waters M. R. and Stafford T. W. 2007. Redefining the Age of Clovis: Implications for the peopling of the Americas. *Science* 315:1122–1126.
- Wittke J. H., Weaver J. C., Bunch T. E., Kennett J. P., Kennett D. J., Moore A. M. T., Hillman G. C., Tankersley K. B., Goodyear A. C., Moore C. R., Daniel I. R., Ray J. H., Lopinot N. H., Ferraro D., Israde-Alcántara I., Bischoff J. L., DeCarli P. S., Hermes R. E., Kloosterman J. B., Revay Z., Howard G. A., Kimbel D. R., Kletetschka G., Nabelek L., Lipo C. P., Sakai S., West A., and Firestone R. B. 2013. Evidence for deposition of 10 million tonnes of impact spherules across four continents 12,800 y ago. *Proceedings of the National Academy of Sciences* 110:E2088–E2097.

SUPPORTING INFORMATION

Additional supporting information may be found in the online version of this article:

Data S1: Detailed description of study sites.